Nonlinear Buckling of Composite Shells of Revolution

Jinsong Huang[1]

Abstract: By adopting the energy method, a method of calculating the stability of the rotational composite shell is presented that takes into account the influence of nonlinear prebuckling deformations and stresses on the buckling of the shell. The relationships between the prebuckling deformations and strains are calculated by nonlinear Karman equations. The numerical method is used to calculate the energy of the whole system. The nonlinear equation is solved by combining the gradient method and the amended Newton iterative method. A computer program is also developed. Examples are given to demonstrate the accuracy of the method presented in this paper.

DOI: 10.1061/(ASCE)0893-1321(2002)15:2(64)

CE Database keywords: Composite materials; Shells; Stability; Buckling.

Introduction

The problems of panel flutter and quasistatic aeroelastic instability (divergence) of composite structures have been intensively studied due to the increasing use of composites in aerospace applications. Outlines of these studies concerning divergence instability have been published by Librescu (1975), several treatises examine the theory of stability, (Brush and Almroth 1975; Kollar and Dulacska 1984), and examples of solving the problems of divergence instability in engineering design have also been published.

Solutions of the problems of statics and dynamics of composite shells and plates, including aeroelastic problems, are usually limited to cylindrical shells; the number of works concerned with the behavior of rotational composite shells is relatively small. FEM (Bushnell 1990; 1984) is widely used for analyzing the behavior of rotational shells, but this paper uses the prebuckling theory and energy variational method to determine the nonlinear stability of a kind of rotational composite shell whose curvature of meridian is monotonic. This kind of shell is widely used in aerospace engineering.

The method presented in this paper takes into account the influence of nonlinear prebuckling deformations and stresses on the buckling of the shell. The relationships between the prebuckling deformations and strains are calculated by using nonlinear Karman equations, and the energy of the system is calculated by using numerical integration. Prebuckling displacements and internal forces are calculated by using the minimum potential energy theory. The linear buckling load P^*(external pressure), F^*(axial compression), and T^*(combination of axial compression and external pressure) are also calculated. The prebuckling deformations and internal forces are calculated by solving the prebuckling equation stepwise at the range of $[0,2P^*]$, $[0,2F^*]$, and $[0,2T^*]$. They are then substituted into the buckling equation to obtain sets of buckling loads and their corresponding buckling wave numbers under the given precision. For each set, buckling loads with the highest precision are obtained by decreasing the step of the iteration; the minimum among all these values is the desired buckling load.

Stiffness of Laminated Composite (Wang 1991)

Consider an anisotropic, heterogeneous double-curved shell in Fig. 1. The thickness of the shell is uniform and denoted by h. The curvilinear orthogonal coordinates 1,2,3 are located on the middle surface. R_1 and R_2 denote the radii of curvature to the middle surface, and α_1 and α_2 are the curvilinear dimensions in 1 and 2 directions, respectively.

$$\begin{Bmatrix} N_1 \\ N_2 \\ N_{12} \\ M_1 \\ M_2 \\ M_{12} \end{Bmatrix} = \begin{bmatrix} A_{11} & A_{12} & A_{16} & B_{11} & B_{12} & B_{16} \\ & A_{22} & A_{26} & B_{12} & B_{22} & B_{26} \\ & & A_{66} & B_{12} & B_{16} & B_{66} \\ & & & D_{11} & D_{12} & D_{16} \\ & & & & D_{22} & D_{26} \\ & & & & & D_{66} \end{bmatrix} \begin{Bmatrix} \epsilon_{10} \\ \epsilon_{20} \\ \gamma_{120} \\ \chi_1 \\ \chi_2 \\ \chi_{12} \end{Bmatrix} \tag{1}$$

where N_1, N_2, and N_{12}=in-plane stress resultants; M_1, M_2, and M_{12}=the stress couples; ϵ_{10}, ϵ_{20}, and γ_{120}=middle surface strain; χ_1, χ_2, and χ_{12}=changes in curvature; $[A]$ represents the values of extensional stiffness; $[D]$ represents the values of bending stiffness; and $[B]$ represents the values of coincidence stiffness between extension and bending. $[A]$, $[B]$, $[C]$ are given as

$$[A_{ij}] = \sum_{k=1}^{n} (\overline{Q}_{ij})_k [h_k - h_{k-1}]$$

$$[B_{ij}] = \frac{1}{2} \sum_{k=1}^{n} (\overline{Q}_{ij})_k [h_k^2 - h_{k-1}^2]$$

$$[D_{ij}] = \frac{1}{3} \sum_{k=1}^{n} (\overline{Q}_{ij})_k [h_k^3 - h_{k-1}^3]$$

where k=number of the lamina; h_k and h_{k-1}=radial coordinates of lamina k; and $(\overline{Q}_{ij})_k$=corresponding transformed stiffness of lamina k.

[1]Associate Professor, College of Water Conservancy and Hydropower Engineering, Wuhan Univ., Wuhan 430072, China.

Note. Discussion open until September 1, 2002. Separate discussions must be submitted for individual papers. To extend the closing date by one month, a written request must be filed with the ASCE Managing Editor. The manuscript for this paper was submitted for review and possible publication on September 6, 2000; approved on August 1, 2001. This paper is part of the ***Journal of Aerospace Engineering***, Vol. 15, No. 2, April 1, 2002. ©ASCE, ISSN 0893-1321/2002/2-64–71/$8.00+$.50 per page.

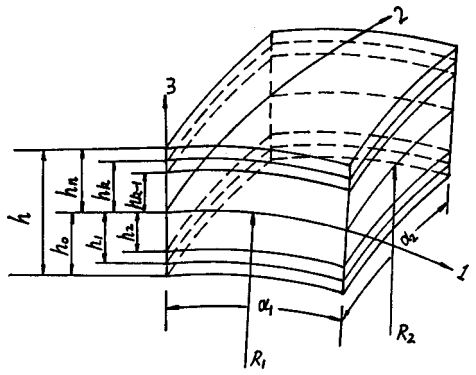

Fig. 1. Geometry and coordinate system of rotational shell

Strain-Displacement Relationships (Fung and Sechlex 1974)

$$\epsilon_{10}=\frac{1}{A_1}\frac{\partial u}{\partial\alpha_1}+\frac{1}{A_1A_2}\frac{\partial A_1}{\partial\alpha_2}v-\frac{w}{R_1}+\frac{1}{2}\left(\frac{1}{A_1}\frac{\partial w}{\partial\alpha_1}\right)^2 \tag{2a}$$

$$\epsilon_{20}=\frac{1}{A_2}\frac{\partial v}{\partial\alpha_2}+\frac{1}{A_1A_2}\frac{\partial A_2}{\partial\alpha_1}u-\frac{w}{R_2}+\frac{1}{2}\left(\frac{1}{A_2}\frac{\partial w}{\partial\alpha_2}\right)^2 \tag{2b}$$

$$\gamma_{120}=\frac{A_1}{A_2}\frac{\partial}{\partial\alpha_2}\left(\frac{u}{A_1}\right)+\frac{A_2}{A_1}\frac{\partial}{\partial\alpha_1}\left(\frac{v}{A_2}\right)+\frac{1}{A_1A_2}\frac{\partial w}{\partial\alpha_1}\frac{\partial w}{\partial\alpha_2} \tag{2c}$$

$$\chi_1=\frac{1}{A_1}\frac{\partial}{\partial\alpha_1}\left(\frac{1}{A_1}\frac{\partial w}{\partial\alpha_1}\right)+\frac{1}{A_1A_2}\frac{\partial A_1}{\partial\alpha_2}\left(\frac{1}{A_2}\frac{\partial w}{\partial\alpha_2}\right) \tag{2d}$$

$$\chi_2=\frac{1}{A_2}\frac{\partial}{\partial\alpha_2}\left(\frac{1}{A_2}\frac{\partial w}{\partial\alpha_2}\right)+\frac{1}{A_1A_2}\frac{\partial A_2}{\partial\alpha_1}\left(\frac{1}{A_1}\frac{\partial w}{\partial\alpha_1}\right) \tag{2e}$$

$$\chi_{12}=\frac{2}{A_1A_2}\left(\frac{\partial^2 w}{\partial\alpha_1\partial\alpha_2}-\frac{1}{A_1}\frac{\partial A_1}{\partial\alpha_2}\frac{\partial w}{\partial\alpha_1}-\frac{1}{A_2}\frac{\partial A_2}{\partial\alpha_1}\frac{\partial w}{\partial\alpha_2}\right) \tag{2f}$$

where A_1 and A_2 are G. Lame coefficients.

Energy Variation Method

Potential energy of the system (Twwey and Marshall 1995):

$$\Pi=\frac{1}{2}\int\int(N_1\epsilon_{10}+N_2\epsilon_{20}+N_{12}\gamma_{120}+M_1\chi_1+M_2\chi_2+M_{12}\chi_{12})A_1A_2d\alpha_1d\alpha_2-\left\{\int\int PwA_1A_2d\alpha_1d\alpha_2+\int\left[N_1^0u+N_{12}^0v-M_1^0\frac{\partial w}{\partial x}+V_1^0w\right]_0^{2\pi}A_2d\alpha_2+\int\left[N_2^0v+N_{12}^0u-M_2^0\frac{\partial w}{\partial y}+V_2^0w\right]_{\varphi_1}^{\varphi_2}A_1d\alpha_1+S^0w|_s\right\} \tag{3}$$

where M_1^0, M_2^0; V_1^0, V_2^0; S^0; $w|_s$ are, respectively, the moment, shear force, wrestle, and angle of torsion given at the edge; P is the external pressure.

The first-order derivative of the strain takes the form

$$\delta\epsilon_{10}=\frac{1}{A_1}\frac{\partial(\delta u)}{\partial\alpha_1}+\frac{1}{A_1A_2}\frac{\partial A_1}{\partial\alpha_2}\delta v-\frac{\delta w}{R_1}+\frac{1}{A_1^2}\frac{\partial w}{\partial\alpha_1}\cdot\frac{\partial(\delta w)}{\partial\alpha_1} \tag{4a}$$

$$\delta\epsilon_{20}=\frac{1}{A_2}\frac{\partial(\delta v)}{\partial\alpha_2}+\frac{1}{A_1A_2}\frac{\partial A_2}{\partial\alpha_1}\delta u-\frac{\delta w}{R_2}+\frac{1}{A_2^2}\frac{\partial w}{\partial\alpha_2}\frac{\partial(\delta w)}{\partial\alpha_2} \tag{4b}$$

$$\delta\gamma_{120}=\frac{A_1}{A_2}\frac{\partial}{\partial\alpha_2}\left(\frac{\delta u}{A_1}\right)+\frac{A_2}{A_1}\frac{\partial}{\partial\alpha_1}\left(\frac{\delta v}{A_2}\right)+\frac{1}{A_1A_2}\frac{\partial w}{\partial\alpha_1}\frac{\partial(\delta w)}{\partial\alpha_2}+\frac{1}{A_1A_2}\frac{\partial w}{\partial\alpha_2}\frac{\partial(\delta w)}{\partial\alpha_1} \tag{4c}$$

$$\delta\chi_1=\frac{1}{A_1}\frac{\partial}{\partial\alpha_1}\left(\frac{1}{A_1}\frac{\partial(\delta w)}{\partial\alpha_1}\right)+\frac{1}{A_1A_2}\frac{\partial A_1}{\partial\alpha_2}\left(\frac{1}{A_2}\frac{\partial(\delta w)}{\partial\alpha_2}\right) \tag{4d}$$

$$\delta\chi_2=\frac{1}{A_2}\frac{\partial}{\partial\alpha_2}\left(\frac{1}{A_2}\frac{\partial(\delta w)}{\partial\alpha_2}\right)+\frac{1}{A_1A_2}\frac{\partial A_2}{\partial\alpha_1}\left(\frac{1}{A_1}\frac{\partial(\delta w)}{\partial\alpha_1}\right) \tag{4e}$$

$$\delta\chi_{12}=\frac{2}{A_1A_2}\left(\frac{\partial^2(\delta w)}{\partial\alpha_1\partial\alpha_2}-\frac{1}{A_1}\frac{\partial A_1}{\partial\alpha_2}\frac{\partial(\delta w)}{\partial\alpha_1}-\frac{1}{A_2}\frac{\partial A_2}{\partial\alpha_1}\frac{\partial(\delta w)}{\partial\alpha_2}\right) \tag{4f}$$

The second-order derivative of the strain takes the form

$$\delta^2\epsilon_{10}=\frac{1}{A_1^2}\left(\frac{\partial(\delta w)}{\partial\alpha_1}\right)^2 \tag{5a}$$

$$\delta^2\epsilon_{20}=\frac{1}{A_2^2}\left(\frac{\partial(\delta w)}{\partial\alpha_2}\right)^2 \tag{5b}$$

$$\delta^2\gamma_{120}=\frac{2}{A_1A_2}\frac{\partial(\delta w)}{\partial\alpha_1}\frac{\partial(\delta w)}{\partial\alpha_2} \tag{5c}$$

Applying the linear stress-strain relation yields the following equations:

$$\delta N_1\epsilon_{10}+\delta N_2\epsilon_{20}+\delta N_{12}\gamma_{120}=N_1\delta\epsilon_{10}+N_2\delta\epsilon_{20}+N_{12}\delta\gamma_{120} \tag{6a}$$

$$\delta M_1\chi_1+\delta M_2\chi_2+\delta M_{12}\chi_{12}=M_1\delta\chi_1+M_2\delta\chi_2+M_{12}\delta\chi_{12} \tag{6b}$$

Substitution of Eq. (6) into the first-order derivative of Eq. (3) yields the following equation:

$$\delta\Pi=\int\int(N_1\delta\epsilon_{10}+N_2\delta\epsilon_{20}+N_{12}\delta\gamma_{120}+M_1\delta\chi_1+M_2\delta\chi_2+M_{12}\delta\chi_{12})A_1A_2d\alpha_1d\alpha_2-\left\{\int\int P\delta wA_1A_2d\alpha_1d\alpha_2+\int\left[N_1^0\delta u+N_{12}^0\delta v-M_1^0\frac{\partial(\delta w)}{\partial x}+V_1^0\delta w\right]_0^{2\pi}A_2d\alpha_2+\int\left[N_2^0\delta v+N_{12}^0\delta u-M_2^0\frac{\partial(\delta w)}{\partial y}+V_2^0\delta w\right]_{\varphi_1}^{\varphi_2}A_1d\alpha_1+S^0\delta w|_s\right\} \tag{7}$$

Let $\delta\Pi=0$. Substitution of Eq. (4) into Eq. (7) yields the equilibrium equations and boundary conditions before buckling.

The second-order derivative of the potential energy of the system is given by

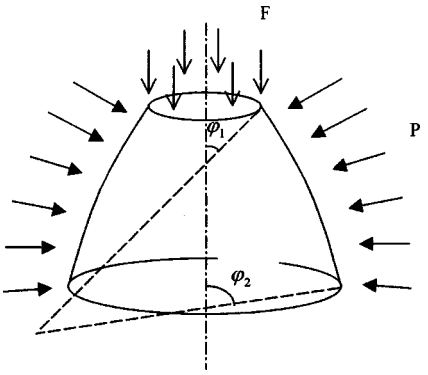

Fig. 2. Loads of rotational shell

$$\delta^2\Pi=\int\int\{[N_1\delta^2\epsilon_{10}+N_2\delta^2\epsilon_{20}+N_{12}\delta^2\gamma_{120}]+[\delta N_1\delta\epsilon_{10}+\delta N_2\delta\epsilon_{20}+\delta N_{12}\delta\gamma_{120}+\delta M_1\delta\chi_1+\delta M_2\delta\chi_2+\delta M_{12}\delta\chi_{12}]\}A_1A_2d\alpha_1d\alpha_2 \tag{8}$$

At the critical point, Eq. (8) takes the form $\delta^2\Pi=0$. Because at the critical point $\delta^2\Pi$ takes the minimum value, to all possible virtual displacement $\delta^*(\delta u)$, $\delta^*(\delta v)$, $\delta^*(\delta w)$ the buckling equations are always: $\delta^*(\delta^2\Pi)=0$.

Prebuckling Analysis

The displacement function before buckling is given as

$$\begin{cases} u=A_0x \\ w=B_0x^2+C_0\sin^2\pi xe^{\beta x} \end{cases} \tag{9}$$

where $x=\varphi-\varphi_1/\varphi_2-\varphi_1$, $\beta=-\sqrt[4]{3(1-\mu^2)R_2^4/R_1^2h^2}$, and A_0, B_0, and C_0 are constants.

Boundary conditions are:

$$\varphi=\varphi_1,\quad x=0,\quad u=0,\quad w=0,\quad \partial w/\partial\varphi=0,\quad x=0,\quad u\neq0,\quad w\neq0;$$

$$\varphi=\varphi_2,\quad x=1,\quad u\neq0,\quad w\neq0$$

where u represents the axial displacement and w represents the normal displacement. The boundary conditions of the rotational shell are defined as a free upper end and a fixed lower end. The chosen displacement functions obviously satisfy the boundary conditions. In the meantime, the displacement functions reflects our assumptions that the axial displacement of the rotational shell is linear and reaches its maximum at the upper end, and the normal displacement is nonlinear and reaches its maximum at the middle of the shell. Note that β is used here to reflect the impact of R_2. Loads are shown in Fig. 2.

Substitution of Eq. (9) into Eq. (2) yields the following equations:

$$\epsilon_{10}=a_{10}A_0+a_{20}B_0+a_{30}C_0+a_{40}B_0^2+a_{50}B_0C_0+a_{60}C_0^2 \tag{10a}$$

$$\epsilon_{20}=b_{10}A_0+b_{20}B_0+b_{30}C_0 \tag{10b}$$

$$\gamma_{120}=0 \tag{10c}$$

$$\chi_1=d_{10}B_0+d_{20}C_0 \tag{10d}$$

$$\chi_1=e_{01}B_0+e_{20}C_0 \tag{10e}$$

$$\chi_{12}=0 \tag{10f}$$

where $a_{i0},b_{i0},d_{i0},e_{i0}\,(i=1,2...)$ are coefficients. Their expressions are given in the appendix.

Substitution of Eq. (10) into Eq. (1) yields the following equations:

$$N_1=Q_{10}A_0+Q_{20}B_0+Q_{30}C_0+Q_{40}B_0^2+Q_{50}B_0C_0+Q_{60}C_0^2 \tag{11a}$$

$$N_2=S_{10}A_0+S_{20}B_0+S_{30}C_0+S_{40}B_0^2+S_{50}B_0C_0+S_{60}C_0^2 \tag{11b}$$

$$M_1=T_{10}A_0+T_{20}B_0+T_{30}C_0+T_{40}B_0^2+T_{50}B_0C_0+T_{60}C_0^2 \tag{11c}$$

$$M_2=P_{10}A_0+P_{20}B_0+P_{30}C_0+P_{40}B_0^2+P_{50}B_0C_0+P_{60}C_0^2 \tag{11d}$$

where $Q_{i0},S_{i0},T_{i0},P_{i0}\,(i=1,2...)$ are coefficients. Their expressions are given in the appendix.

Substitution of Eqs. (10) and (11) into Eq. (3) yields the following equations:

$$\Pi=\int\int\lambda_1A_0^2+\lambda_2B_0^2+\lambda_3C_0^2+\lambda_4A_0B_0+\lambda_5A_0C_0+\lambda_6B_0C_0+\lambda_7B_0^3+\lambda_8C_0^3+\lambda_9A_0B_0^2+\lambda_{10}A_0C_0^2+\lambda_{11}B_0^2C_0+\lambda_{12}B_0C_0^2+\lambda_{13}A_0B_0C_0+\lambda_{14}B_0^4+\lambda_{15}C_0^4+\lambda_{16}B_0^2C_0^2+\lambda_{17}B_0^3C_0+\lambda_{18}B_0C_0^3)A_1A_2d\alpha_1d\alpha_2-\left\{\int\int(\lambda_{19}B_0+\lambda_{20}C_0)PA_1A_2d\alpha_1d\alpha_2+\int(\lambda_{21}A_0+\lambda_{22}B_0)FA_2d\alpha_2 \right. \tag{12}$$

where the expressions for $\lambda_i\,(i=1,22)$ are given in the appendix.

Now, applying the minimum potential energy theory:

$$\frac{\partial(\Pi)}{\partial A_0}=0;\quad \frac{\partial(\Pi)}{\partial B_0}=0;\quad \frac{\partial(\Pi)}{\partial C_0}=0 \tag{13}$$

Displacements and the internal forces before buckling can be obtained by solving the above Eq. (13).

Buckling Analysis

The buckling displacement function is given as

$$\begin{cases} \delta u=A\cos m\pi x\sin n\theta \\ \delta v=B\sin m\pi x\cos n\theta \\ \delta w=C\sin m\pi x\sin n\theta \end{cases} \tag{14}$$

where A, B, and C are constants. Boundary conditions are $\varphi=\varphi_1$, $x=0$, $v=0$; $\varphi=\varphi_2$, $x=1$, $v=0$.

Substitution of Eq. (14) into Eqs. (4) and (5) yields the following equations:

$$\delta\epsilon_{10}=a_1A+a_2C+a_3B_0C+a_4C_0C \tag{15a}$$

$$\delta\epsilon_{20}=b_1A+b_2B+b_3C \tag{15b}$$

$$\delta\epsilon_{120}=d_1A+d_2B+d_3B_0C+d_4C_0C \tag{15c}$$

$$\delta\chi_1=e_1C \tag{15d}$$

$$\delta\chi_1=f_1C \tag{15e}$$

$$\delta\chi_{12}=g_1C \tag{15f}$$

$$\delta^2\epsilon_{10}=j_1C^2 \tag{15g}$$

$$\delta^2\epsilon_{20}=k_1C^2 \tag{15h}$$

$$\delta^2\epsilon_{120}=l_1C^2 \tag{15i}$$

where $a_i, b_i, d_i, e_i, f_i, g_i, j_i, k_i, l_i\ (i=1,2...)$ are coefficients. Their expressions are given in the appendix.

Substitution of Eq. (15) into Eq. (1) yields the following equations:

$$\delta N_1=Q_1A+Q_2B+Q_3B_0C+Q_4C_0C+Q_5C \tag{16a}$$

$$\delta N_2=S_1A+S_2B+S_3C+S_4B_0C+S_5C_0C \tag{16b}$$

$$\delta N_{12}=T_1A+T_2B+T_3C+T_4B_0^2C+T_5C_0C \tag{16c}$$

$$\delta M_1=H_1A+H_2B+H_3C+H_4B_0C+T_5C_0C \tag{16d}$$

$$\delta M_2=P_1A+P_2B+P_3C+P_4B_0C+P_5C_0C \tag{16e}$$

$$\delta M_{12}=F_1A+F_2B+F_3C+F_4B_0C+F_5C_0C \tag{16f}$$

where $Q_i, S_i, T_0, H_I, P_i, F_i\ (i=1,2...)$ are coefficients. Their expressions are given in the appendix.

Substitution of Eqs. (15) and (16) into Eq. (8) yields the following equations:

$$\delta^2\Pi=\int\int\{[N_1\xi_1C^2+N_2\xi_2C^2+N_{12}\xi_3C^2]+[\xi_4A^2+\xi_5B^2+\xi_6C^2+\xi_7AB+\xi_8AC+\xi_9BC]\}A_1A_2d\alpha_1d\alpha_2 \tag{17}$$

where $\xi_i\ (i=1,2,...)$ are coefficients. Their expressions are given in the appendix. Calculating δ^* variation of Eq. (17) yields the buckling equations.

Solving Technique

First, linear buckling loads P^*(external pressure), F^*(axial compression), and T^*(combination of axial compression and external pressure) are calculated. Second, the prebuckling deformations and internal forces are calculated by solving the prebuckling equation stepwise at the range of $[0,2P^*]$, $[0,2F^*]$, and $[0,2T^*]$. They are then substituted into the buckling equation to obtain sets of buckling loads and their corresponding buckling wave numbers under the given precision. For each set, buckling loads with the highest precision are obtained by decreasing the step of the iteration; the minimum among all these values is the desired buckling load.

A computer program is developed in *FORTRAN*. The integral is evaluated numerically by Monte Carlo formula. The gradient method and the amended Newton iterative method are combined to solve the nonlinear equations. The gradient method is used to assign the initial value, and the Newton iterative method is used to increase the precision.

Examples

Example 1 is taken from Wang (1991). The shell is cylindrical with length=500 mm; radius=500 mm; thickness of single layer =0.15 mm; Young's modulus=117.6 Gpa(major), 5.88 Gpa(minor); shear modulus=2.94 GPa, and Poisson's ratio=0.3. The types of laminates are defined as

Table 1. Cylindrical Shell under External Pressure Unit: MPa

Type	Shear theory (Wang 1991)	Classic theory (Wang 1991)	Method in this paper	Method in this paper[a]
1	0.590(1,7)	0.605(1,7)	0.589323(1,7)	0.589323(1,7)
2	0.627(1,8)	0.645(1,8)	0.560094(1,7)	0.632145(1,8)
3	0.0976(1,9)	0.0990(1,9)	0.086167(1,8)	0.0986224(1,9)
4	0.336(1,11)	0.342(1,11)	0.322148(1,10)	0.339241(1,11)
5	0.0527(1,13)	0.0531(1,13)	0.047492(1,12)	0.052912(1,13)

[a]Results are obtained by restricting the half-wave magnitudes to be the same as their corresponding ones in the second column.

1. Perpendicular symmetrical, 40 layers;
2. ±45° symmetrical, 40 layers;
3. ±45° symmetrical, 20 layers;
4. ±22.5° symmetrical, 40 layers; and
5. ±22.5° symmetrical, 20 layers.

The results of critical loads and half-wave magnitudes are given in Table 1. Since the shell is cylindrical, R_1=infinity, theoretically. In this paper, a very big value of 100,000 mm is assigned to R_1 for calculation.

The critical loads given by the method of this paper (see fourth column in Table 1) are lower than those based on a shearable shell model (see second column). For types 2 to 5, the half-wave magnitudes calculated by the method of this paper (see fourth column) are also lower than those from Wang (1991) (see second column). The model presented in this paper is unshearable; however, it takes the prebuckling deformation and stress into account. Comparison of the results shows that the prebuckling deformation and stress reduce the stabilities of the shells. When the half-wave magnitudes are restricted to be the same as their corresponding ones in the second column, the predicted critical loads in this paper (see fifth column) are somewhere between the critical loads given by the shear theory (see second column) and the critical loads given by the classic theory (see third column). The results imply that the shells would actually buckle at the lower-order models (the half-wave magnitudes decrease) when the prebuckling deformation and stress are taken into account.

Example 2 uses the program developed according to the theoretical model of this paper. The stability of a submarine-launched missile's composite dome under external pressure is calculated. The structural contour of the fairing studied in this paper is a rotational thin shell that consists of a long, thin shell structure and a short, cylindrical shell structure (transitional part). The main body of the structure is made of seven-ply laminated woods. Longitudinal-direction layers of wood alternates with transverse-direction layers of wood from the outer to the inner surface of the shell. The ends of the shell are made of aluminum, as shown in Fig. 3(a). This kind of structural model has been applied to many actual engineering structures. The material properties of the wood are thickness of single layer=0.5 mm; Young's modulus=10.416 Gpa(major), 1.644 Gpa(minor); shear modulus=1.6 GPa; and Poisson's ratio=0.343. The boundary conditions are fix-supported (all the degrees of freedom are restrained) at the top, and roller-supported (all the degrees of freedom are restrained except for the vertical degree of freedom) at the bottom.

The critical external pressure calculated by using the developed program of the dome is 0.0343 MPa. In order to analyze the stability of the dome, several parameters are changed to recalculate the critical loads. The calculated results are shown in Figs. 4–7. In these figures P_{cr}=the critical load and the unit =MPa; R_1, R_x, L, and t, are shown in Fig. 3(b) (R_x represents the top horizontal radius; the horizontal radius of the lower end is

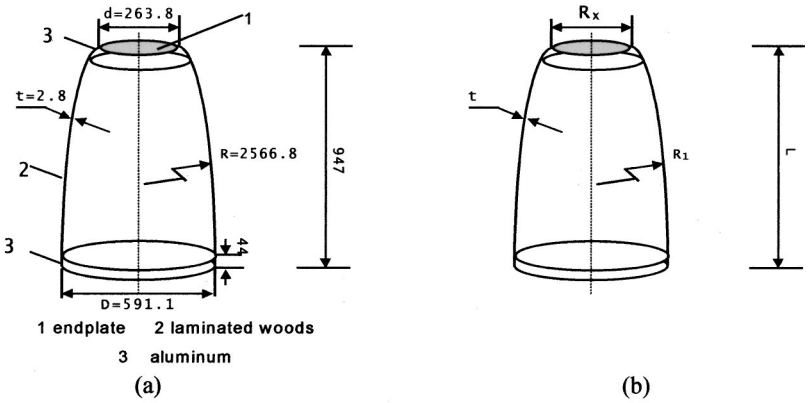

Fig. 3. Contour of fairing (unit=mm)

also changed using the same scale); and R_{10}, R_{x0}, L_0, and t_0 are their initial values, respectively. Based on the calculated results, conclusions can be drawn that the stability of the dome under external pressure can be enhanced by diminishing R_1 in a certain range or increasing t. The stability of the dome decays if the value of L or R_x is increased.

Different types of laminates are used to recalculate the critical loads. Results are shown in Table 2. It can be seen that increasing the transverse-direction layer number can enhance the stability of the dome under external pressure, where 0 represents the longitudinal-direction layer; 90 represents the transverse-direction layer; 45 represents the angle between the axis of the laminate

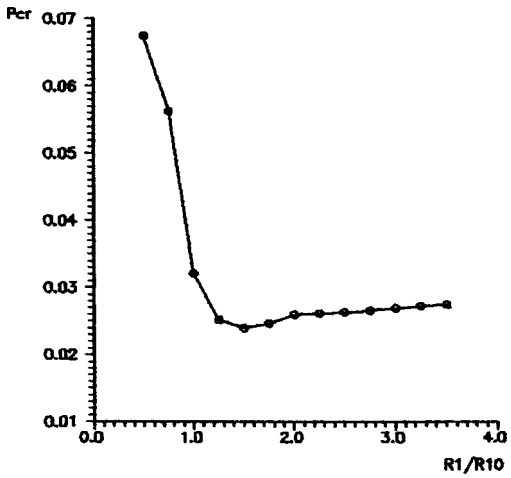

Fig. 4. Relation between critical load and R_1

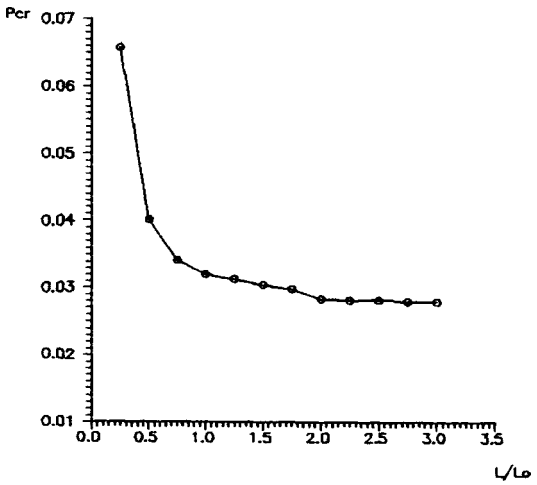

Fig. 6. Relation between critical load and L

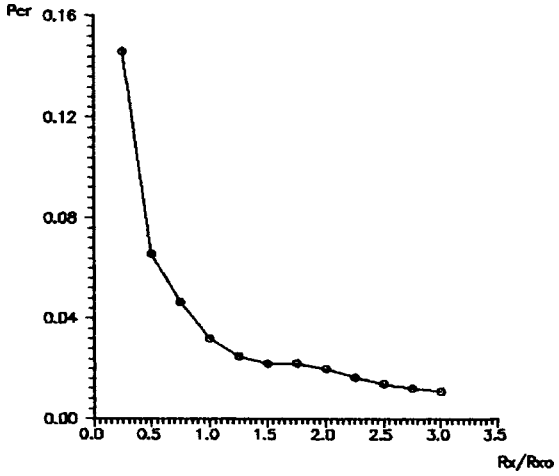

Fig. 5. Relation between critical load and R_x

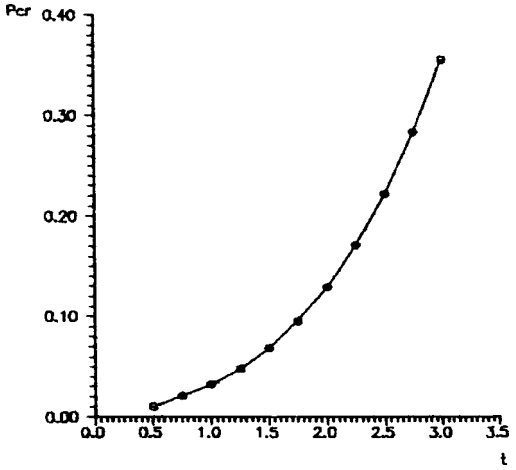

Fig. 7. Relation between critical load and t

Table 2. Dome under External Pressure

Case	Type of laminates	Critical loads (MPa)
1	(90,0,90,0,90,0,90)	0.039287
2	(90,0,90,0,90)	0.040641
3	(0,90,0,90,0,90,0)	0.032060
4	(45,−45,45,−45,45,−45,45)	0.041283
5	(90,90,0,90,0,90,90)	0.042268
6	(0,0,90,0,90,0,0)	0.028885
7	(90,90,90,90,90,90,90)	0.041001
8	(0,0,0,0,0,0,0)	0.029808

and the longitudinal axis of the dome(clockwise); and −45 represents the angle between the axis of the laminate and the longitudinal axis of the dome (counterclockwise). In Case 2, the thickness of the single layer is 0.7 mm, and the thickness of the laminates=3.5 mm. In Cases 1 and 3 through 8, the thickness of the single layer=0.5 mm, and the thickness of the laminates=3.5 mm.

Conclusion

This paper presents a method to determine the nonlinear stability of the specific rotational composite shells that are widely used in aerospace engineering. It proves that prebuckling deformation and stress reduce the stabilities of a rotational composite shell, and the shell would actually buckle at a lower-order model (the half-wave magnitudes decrease) when the prebuckling deformation and stress are taken into account. This method is applicable for calculating the buckling loads of a rotational shell whose curvature of meridian is monotonic. Due to the simplicity of data gathering and preparation required by the proposed method, the model presented in this paper is especially useful when it is necessary to make a quick decision from several designed options.

The stability of a submarine-launched missile's composite dome (Fig. 3) under external pressure is calculated by the FORTRAN program based on the theoretical model in this paper. The calculated result shows that the stability of the dome can be enhanced by diminishing R_1 in a certain range, increasing the transverse-direction layer number, or increasing the t value. It also suggests that the stability of the dome diminishes if the value of L or R_x is increased.

Appendix

The following expressions are for coefficients in Eq. (10):

$$a_{10}=-\frac{1}{R_1(\varphi_2-\varphi_1)}$$

$$a_{20}=-\frac{x^2}{R_1}$$

$$a_{30}=-\frac{1}{R_1}\sin^2\pi x e^{\beta x}$$

$$a_{40}=\frac{2x^2}{R_1^2(\varphi_2-\varphi_1)^2}$$

$$a_{50}=\frac{2x}{R_1^2(\varphi_2-\varphi_1)^2}(2\pi\sin\pi x\cos\pi x e^{\beta x}+\beta e^{\beta x}\sin^2\pi x)$$

$$a_{60}=\frac{1}{2R_1^2(\varphi_2-\varphi_1)^2}(2\pi\sin\pi x\cos\pi x e^{\beta x}+\beta e^{\beta x}\sin^2\pi x)^2$$

$$b_{10}=\frac{ctg\varphi}{R_1}x$$

$$b_{20}=-\frac{x^2}{R_2}$$

$$b_{30}=-\frac{\sin^2\pi x e^{\beta x}}{R_2}$$

$$d_{10}=\frac{2}{R_1^2(\varphi_2-\varphi_1)^2}$$

$$d_{20}=\frac{e^{\beta x}}{R_1^2(\varphi_2-\varphi_1)^2}[2\pi^2(\cos^2\pi x-\sin^2\pi x)$$

$$+4\pi\beta\sin\pi x\cos\pi x\beta+\beta^2\sin^2\pi x]$$

$$e_{20}=-\frac{2xctg\varphi}{R_1^2(\varphi_2-\varphi_1)}$$

$$e_{20}=-\frac{ctg\varphi}{R_1^2(\varphi_2-\varphi_1)}(2\pi\sin\pi x\cos\pi x e^{\beta x}+\beta\sin^2\pi x e^{\beta x})$$

The following expressions are for coefficients in Eq. (11):

$$Q_{10}=A_{11}a_{10}+A_{12}b_{10}$$

$$Q_{20}=A_{11}a_{20}+A_{12}b_{20}+B_{11}d_{10}+B_{12}e_{10}$$

$$Q_{30}=A_{11}a_{30}+A_{12}b_{30}+B_{11}d_{20}+B_{12}e_{20}$$

$$Q_{40}=A_{11}a_{40}$$

$$Q_{50}=A_{11}a_{50}$$

$$Q_{60}=A_{11}a_{60}$$

$$S_{10}=A_{12}a_{10}+A_{22}b_{10}$$

$$S_{20}=A_{12}a_{20}+A_{22}b_{20}+B_{12}d_{10}+B_{22}e_{10}$$

$$S_{30}=A_{12}a_{30}+A_{22}b_{30}+B_{12}d_{20}+B_{22}e_{20}$$

$$S_{40}=A_{12}a_{40}$$

$$S_{50}=A_{12}a_{50}$$

$$S_{60}=A_{12}a_{60}$$

$$T_{10}=B_{11}a_{10}+B_{12}b_{10}$$

$$T_{20}=B_{11}a_{20}+B_{12}b_{20}+D_{11}d_{10}+D_{12}e_{10}$$

$$T_{30}=B_{11}a_{30}+B_{12}b_{30}+B_{11}d_{20}+B_{12}e_{20}$$

$$T_{40}=B_{11}a_{40}$$

$$T_{50}=B_{11}a_{50}$$

$$T_{60}=B_{11}a_{60}$$

$$P_{10}=B_{12}a_{10}+B_{22}b_{10}$$

$$P_{20}=B_{12}a_{20}+B_{22}b_{20}+D_{12}d_{10}+D_{22}e_{10}$$

$$P_{30}=B_{12}a_{30}+B_{22}b_{30}+D_{12}d_{20}+D_{22}e_{20}$$

$$P_{40}=B_{12}a_{40}$$

$$P_{50}=B_{12}a_{50}$$

$$P_{60}=B_{12}a_{60}$$

The following expressions are for coefficients in Eq. (12):

$$\lambda_1=Q_{10}d_{10}+S_{10}b_{10}$$

$$\lambda_2=Q_{20}a_{20}+S_{20}b_{20}+T_{20}d_{10}+P_{20}e_{10}$$

$$\lambda_3=Q_{30}a_{30}+S_{30}b_{30}+T_{30}d_{20}+P_{30}e_{20}$$

$$\lambda_4=Q_{20}a_{10}+Q_{10}a_{20}+S_{10}b_{20}+S_{20}b_{10}+T_{10}d_{10}+P_{10}e_{10}$$

$$\lambda_5=Q_{30}a_{10}+Q_{10}a_{30}+S_{30}b_{10}+S_{10}b_{30}+T_{10}d_{20}+P_{10}e_{20}$$

$$\lambda_6=Q_{30}a_{20}+Q_{20}a_{30}+S_{30}b_{20}+S_{20}b_{30}+T_{30}d_{10}+T_{20}d_{20}+P_{30}e_{10}+P_{20}e_{20}$$

$$\lambda_7=Q_{40}a_{20}+Q_{20}a_{40}+S_{40}b_{20}+T_{40}d_{10}+P_{40}e_{10}$$

$$\lambda_8=Q_{60}a_{30}+Q_{30}a_{60}+S_{60}b_{30}+T_{60}d_{20}+P_{60}e_{20}$$

$$\lambda_9=Q_{40}a_{10}+Q_{10}a_{40}+S_{40}b_{10}$$

$$\lambda_{10}=Q_{60}a_{10}+Q_{10}a_{60}+S_{60}b_{10}$$

$$\lambda_{11}=Q_{50}a_{20}+Q_{20}a_{50}+Q_{40}a_{30}+Q_{30}a_{40}+S_{50}b_{20}+S_{40}b_{30}+T_{50}d_{10}+T_{40}d_{20}+P_{50}e_{10}+P_{40}e_{20}$$

$$\lambda_{12}=Q_{60}a_{20}+Q_{50}a_{30}+Q_{30}a_{50}+Q_{20}a_{60}+S_{60}b_{20}+S_{50}b_{30}+T_{60}d_{10}+T_{50}d_{20}+P_{60}e_{10}+P_{50}e_{20}$$

$$\lambda_{13}=Q_{50}a_{10}+Q_{10}a_{50}+S_{50}b_{10}$$

$$\lambda_{14}=Q_{40}a_{40}$$

$$\lambda_{15}=Q_{60}a_{60}$$

$$\lambda_{16}=Q_{50}a_{50}+Q_{60}a_{40}+Q_{40}a_{60}$$

$$\lambda_{17}=Q_{50}a_{40}+Q_{40}a_{50}$$

$$\lambda_{18}=Q_{60}a_{50}+Q_{50}a_{60}$$

$$\lambda_{19}=x^2$$

$$\lambda_{20}=\sin^2\pi x e^{\beta x}$$

$$\lambda_{21}=\sin\varphi_1$$

$$\lambda_{22}=-\cos\varphi_1$$

The following expressions are for coefficients in Eq. (15):

$$a_1=\frac{m\pi}{R_1(\varphi_2-\varphi_1)}\sin m\pi x\sin n\theta$$

$$a_2=-\frac{1}{R_1}\sin m\pi x\sin n\theta$$

$$a_3=\frac{2m\pi x}{R_1^2(\varphi_2-\varphi_1)^2}\cos m\pi x\sin n\theta$$

$$a_4=\frac{m\pi}{R_1^2(\varphi_2-\varphi_1)^2}(2\pi\sin\pi x\cos\pi x e^{\beta x}+\beta\sin^2\pi x e^{\beta x})\cos m\pi x\sin n\theta$$

$$b_1=\frac{ctg\varphi}{R_1}\cos m\pi x\sin n\theta$$

$$b_2=-\frac{n}{R_2\sin\varphi}\sin m\pi x\sin n\theta$$

$$b_3=-\frac{1}{R_2}\sin m\pi x\sin n\theta$$

$$d_1=\frac{n}{R_2\sin\varphi}\cos m\pi x\cos n\theta$$

$$d_2=\left(\frac{ctg\varphi}{R_1}\sin m\pi x\cos n\theta+\frac{m\pi}{R_1(\varphi_2-\varphi_1)}\cos m\pi x\cos n\theta\right)$$

$$d_3=-\frac{2nx}{R_1R_2(\varphi_2-\varphi_1)\sin\varphi}\sin m\pi x\cos n\theta$$

$$d_4=-\frac{2\pi\sin\pi x\cos\pi x e^{\beta x}+\beta\sin^2\pi x e^{\beta x}}{R_1R_2(\varphi_2-\varphi_1)\sin\varphi}\sin m\pi x\cos n\theta$$

$$e_1=-\frac{m^2\pi^2}{R_1^2(\varphi_2-\varphi_1)^2}\sin m\pi x\sin n\theta$$

$$f_1=-\frac{m\pi ctg\varphi}{R_1^2(\varphi_2-\varphi_1)}\cos m\pi x\sin n\theta-\frac{n^2}{R_2^2\sin^2\varphi}\sin m\pi x\sin n\theta$$

$$g_1=-\frac{2}{R_1R_2\sin\varphi}\left(\frac{\pi mn}{\varphi_2-\varphi_1}\cos m\pi x\cos n\theta+nctg\varphi\sin m\pi x\cos n\theta\right)$$

$$j_1=\left(\frac{m\pi}{R_1(\varphi_2-\varphi_1)}\cos m\pi x\sin n\theta\right)^2$$

$$k_1=\left(\frac{n\sin m\pi x\cos n\theta}{R_2\sin\varphi}\right)^2$$

$$l_1=\frac{2mn\pi}{R_1R_2(\varphi_2-\varphi_1)\sin\varphi}\sin m\pi x\cos m\pi x\sin n\theta\cos n\theta$$

The following expressions are for coefficients in Eq. (16):

$$Q_1=A_{11}a_1+A_{12}b_1+A_{16}d_1$$

$$Q_2=A_{12}b_2+A_{16}d_2$$

$$Q_3=A_{11}a_3+A_{16}d_3$$

$$Q_4=A_{11}a_4+A_{16}d_4$$

$$Q_5=A_{11}a_2+A_{12}b_3+B_{11}e_1+B_{12}f_1+B_{16}g_1$$

$$S_1=A_{12}a_1+A_{22}b_1+A_{26}d_1$$

$$S_2=A_{12}b_2+A_{26}d_2$$

$$S_3=A_{12}a_2+A_{22}b_3+B_{12}e_1+B_{22}f_1+B_{26}g_1$$

$$S_4=A_{12}a_3+A_{26}d_3$$

$$S_5=A_{12}a_4+A_{26}d_4$$

$$T_1=A_{16}a_1+A_{26}b_1+A_{66}d_1$$

$$T_2=A_{26}b_2+A_{66}d_2$$

$$T_3=A_{16}a_2+A_{26}b_3+B_{16}e_1+B_{26}f_1+B_{66}g_1$$

$$T_4=A_{16}a_3+A_{66}d_3$$

$$T_5=A_{16}a_4+A_{66}d_4$$

$$H_1=B_{11}a_1+B_{12}b_1+B_{16}d_1$$

$$H_2=B_{12}b_2+B_{16}d_2$$

$$H_3 = B_{11}a_2 + B_{12}b_3 + D_{11}e_1 + D_{12}f_1 + D_{16}g_1$$

$$H_4 = B_{11}a_3 + B_{16}d_3$$

$$H_5 = B_{11}a_4 + B_{16}d_4$$

$$P_1 = B_{12}a_1 + B_{22}b_1 + B_{26}d_1$$

$$P_2 = B_{22}b_2 + B_{26}d_2$$

$$P_3 = B_{12}a_2 + B_{22}b_3 + D_{12}e_1 + D_{22}f_1 + D_{26}g_1$$

$$P_4 = B_{12}a_3 + B_{26}d_3$$

$$P_5 = B_{12}a_4 + B_{26}d_4$$

$$F_1 = B_{16}a_1 + B_{26}b_1 + B_{66}d_1$$

$$F_2 = B_{26}b_2 + B_{66}d_2$$

$$F_3 = B_{16}a_2 + B_{26}b_3 + D_{16}e_1 + D_{26}f_1 + D_{66}g_1$$

$$F_4 = B_{16}a_3 + B_{66}d_3$$

$$F_5 = B_{16}a_4 + B_{66}d_4$$

The following expressions are for coefficients in Eq. (17):

$$\xi_1 = j_1$$

$$\xi_2 = k_1$$

$$\xi_3 = l_1$$

$$\xi_4 = Q_1a_1 + S_1b_1 + T_1d_1$$

$$\xi_5 = S_2b_2 + T_2d_2$$

$$\xi_6 = Q_3a_2 + S_3b_3 + H_3e_1 + P_3f_1 + F_3g_1 + B_0(Q_4a_2 + Q_3a_3 + S_4b_3 + T_3d_3 + H_4e_1 + P_4f_1 + F_4g_1) + C_0(Q_5a_2 + Q_3a_4 + S_5b_3 + T_3d_4 + H_5e_1 + P_5f_1 + F_5g_1) + B_0C_0(Q_5a_3 + Q_4a_4 + T_5d_3 + T_4d_4) + B_0^2(Q_4a_3 + T_4d_3) + C_0^2(Q_5a_4 + T_5d_4)$$

$$\xi_7 = Q_2a_1 + S_1b_2 + S_2b_1 + T_2d_1 + T_1d_2$$

$$\xi_8 = Q_3a_1 + Q_1a_2 + S_1b_3 + S_3b_1 + T_3d_1 + H_1e_1 + P_1f_1 + F_1g_1 + B_0(Q_4a_1 + Q_1a_3 + S_4b_1 + T_4d_1 + T_1d_3) + C_0(Q_5a_1 + Q_1a_4 + S_5b_1 + T_5d_1 + T_1d_4)$$

$$\xi_9 = Q_2a_2 + S_3b_2 + S_2b_3 + T_3d_2 + H_2e_1 + P_2f_1 + F_2g_1 + B_0(Q_2a_3 + S_4b_2 + T_4d_2 + T_2d_3) + C_0(Q_2a_4 + S_5b_2 + T_5d_2 + T_2d_4)$$

References

Brush, D. D., and Almroth, B. O. (1975). *Buckling of bars, plates, and shells*, McGraw-Hill, New York.

Bushnell, D. (1970). ''Analysis of buckling and vibration of ring-stiffened, segmented shells of revolution.'' *Int. J. Solids Struct.*, 6(2), 157–181.

Bushnell, D. (1984). ''Computerized analysis of shell-governing equations.'' *Comput. Struct.*, 18(3), 471–536.

Fung, Y. C., and Sechlex, E. E. (1974). *Thin-shell structures—Theory, experiment and design*, Prentice-Hall, Englewood Cliffs, N.J.

Kollar, L., and Dulacska, E. (1984). *Buckling of shells for engineering*, Wiley, New York.

Librescu, L. (1975). *Elastostatics and kinetics of anisotropic and heterogeneous shell-type structures*, Noordhoff International, Leyden, The Netherlands.

Twwey, G. J., and Marshall, L. H. (1995). *Buckling and postbuckling of composite plates*, Chapman & Hall, London.

Wang, Z. (1991). *Mechanics and structural mechanics of composite materials*, Mechanical Industry, Beijing (in Chinese), 105–108, 418–420.